J. Fluid Mech. (1979), *vol.* 90, *part* 2, *pp.* 327–336
Printed in Great Britain

Wave-tank experiments on an immersed parallel-plate duct

By G. F. KNOTT AND J. O. FLOWER
School of Engineering and Applied Sciences, University of Sussex,
Falmer, Brighton BN1 9QT, England

(Received 22 May 1978)

A series of experiments is described in which a fully submerged parallel-plate enclosure is subjected to regular incident waves. The resulting wave-interaction effects are defined in terms of a reflexion coefficient derived from wave-height measurements and a pressure coefficient derived from measurements of pressure in the depths of the enclosure. The latter parameter describes the pressure induced in the enclosure by the passage of regular waves above it and is of particular interest, at present, in having a bearing on the operation and performance of a sub-sea wave-energy converter currently under development. The outcome of these experiments is the partial verification of some recent theoretical work, including the demonstration of a pressure intensification at certain wave frequencies.

These experiments form part of a wider study concerned generally with the performance of immersed, pressure-driven, wave-energy converters.

1. Introduction

A device has recently been proposed for wave-energy conversion which operates entirely beneath the surface (see, for example, Lighthill 1979). In principle, a gravitationally balanced fluid column contained within a U-shaped duct is forced to oscillate resonantly in response to wave-induced pressures at its mouth. One end of the tube is open to ambient conditions and the other to a constant-pressure air reservoir; see figure 1.

The dynamics of the system can conveniently be divided into two parts: the internal dynamics, which relate to the mechanical properties of the fluid column, and the external dynamics, which concern the manner in which the enclosure as a whole interacts with the neighbouring wave field. The former can be simplified to a damped mass/spring system but the latter has no such simple representation, and it is the comparative absence of practical knowledge about this coupled with the recent appearance of a theoretical treatment by Lighthill (1979) which has prompted the present investigation. The theoretical treatment presented by Lighthill concerns two cases, both of which are two-dimensional in nature. In the first, pressures and reflexions are calculated for a deep parallel-plate enclosure in which no oscillatory flow is allowed to occur; in the second, a more complex dynamical analysis is performed on a duct in which the entrained fluid is allowed to oscillate in response to wave-induced pressures. In the latter case, the damped response of the system is calculated, thus combining both aspects of the dynamical model. The present work is, however, confined to the simpler case in that it concerns only the 'infinite' parallel-plate situation.

Additional material on this subject, concerned with scattering from immersed plates, can be found in an earlier paper by Jarvis (1971).

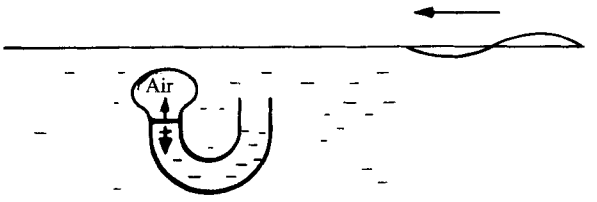

FIGURE 1. Simple representation of the immersed U-tube wave-energy device currently under development by Messrs Vickers Ltd.

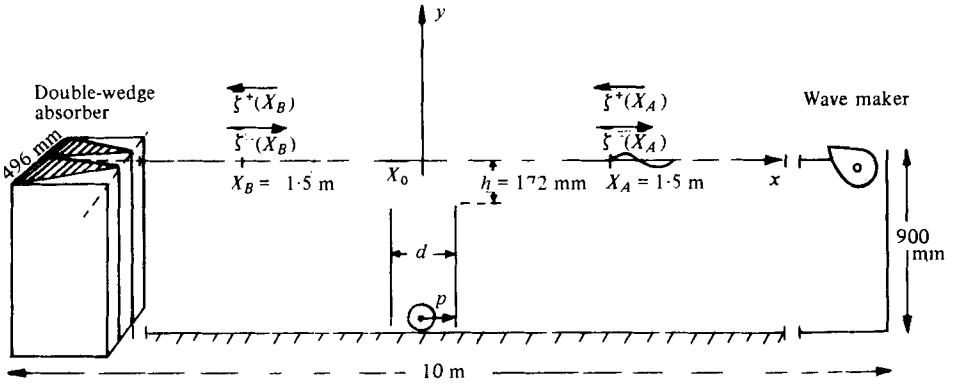

FIGURE 2. Schematic diagram of the apparatus.

2. Parameters of interest and the basic experiment

The duct, open at the top and consisting essentially of two parallel plates, was set in the mid-section of a wave tank as illustrated in figure 2. Constant-period waves were propagated along the channel and, after sufficient time had elapsed for settling, wave-height recordings were made at four stations (two pairs either side of the duct). From these, the amplitude and phase of the direct and reflected wave trains on both sides of the duct can be deduced (see appendix for method of derivation); simultaneously, a measurement was also made of the oscillating pressure in the enclosure. From these wave and pressure measurements four quantities were derived, namely, the pressure-amplification ratio K, duct reflexion coefficient R, pressure phase lag α_p and wave phase lag α_ζ.

2.1. *Pressure-amplification ratio*

This parameter is derived from the equation

$$K = |p|/\rho g \exp(-kh)\,|\zeta^+(X_A)^* + \zeta^-(X_B)^*|,$$

which relates the magnitude of the oscillating pressure p experienced in the depths of the duct to the magnitude which would be experienced at the level of the duct mouth owing to the incident waves if the duct were removed. The exact symmetry of the system allows the influence of tank reflexions to be accounted for; these varied between 2 and 5 % of the direct wave. The denominator of K, being the pressure due to the incident waves, is derived from the vector sum of the two sets of incident waves (i.e. those coming from the wave maker, $\zeta^+(X_A)$, and those from the beach, $\zeta^-(X_B)$) after

both have been translated to an origin at the centre of the enclosure using linear deep-water theory (this transfer entails a simple phase shift and is indicated by an asterisk). The vector summation is required since the waves

$$\zeta^+(x) = A\sin(\omega t + kx + \phi_A), \quad \zeta^-(x) = B\sin(\omega t - kx + \phi_B)$$

are defined in both amplitude and phase, and due regard must be paid to their manner of combination. In terms of magnitude and phase, the translated waves are given by

$$|\zeta^+(X_A)^*| = |\zeta^+(X_A)|, \quad \text{ph}\,[\zeta^+(X_A)^*] = \text{ph}\,[\zeta^+(X_A)] - (2\pi f)^2(X_A - X_0)/g,$$

$$|\zeta^-(X_B)^*| = |\zeta^-(X_B)|, \quad \text{ph}\,[\zeta^-(X_B)^*] = \text{ph}\,[\zeta^-(X_B)] + (2\pi f)^2(X_0 - X_B)/g,$$

where $f\,(Hz)$ is the wave frequency.

2.2. *Reflexion coefficient*

This is defined as the square of the ratio of the amplitudes of the reflected and incident waves. Numerically,

$$R = |\zeta^-(X_A) - \zeta^-(X_B)^{**}|^2/|\zeta^+(X_A)|^2,$$

where

$$|\zeta^-(X_B)^{**}| = |\zeta^-(X_B)|\,|\zeta^+(X_B)|/|\zeta^+(X_A)|,$$

$$\text{ph}\,[\zeta^-(X_B)^{**}] = \text{ph}\,[\zeta^-(X_B)] - (2\pi f)^2(X_A - X_B)/g - \alpha_\zeta.$$

In this paper the reflexion coefficient represents the proportion of the incident *wave energy* which is reflected back from the cavity. This factor has been corrected, as has K, for the influence of tank reflexions, which were of the same order of magnitude as the duct reflexion itself. To account for this, the measured transmission characteristics of the duct are used to translate the tank reflexions $\zeta^-(X_B)$ measured at X_B to X_A, where they are subtracted vectorially from the total measured reflexions $\zeta^-(X_A)$, leaving the reflexions attributable solely to the duct itself (this origin shift is indicated by the superscript **). The remaining error is thereby reduced to a second-order effect.

2.3. *Pressure phase lag*

This factor represents the angle by which the pressure in the depths of the duct lags in phase from the incident wave (actually the vector sum of the two incident waves):

$$\alpha_p = \text{ph}\,[\zeta^+(X_A)^* + \zeta^-(X_B)^*] - \text{ph}\,p.$$

2.4. *Wave phase lag*

This factor represents the angle by which the phase of the transmitted wave lags that of the incident wave:

$$\alpha_\zeta = \text{ph}\,[\zeta^+(X_A)^*] - \text{ph}\,[\zeta^+(X_B)^*].$$

3. Testing and equipment

The testing was carried out in the wave tank in the School of Engineering and Applied Sciences at the University of Sussex. The principal dimensions of the tank are $10 \times 0{\cdot}5 \times 0{\cdot}9$ m (figure 2). At one end of the tank waves were generated by the servo-driven wave maker, based on a Salter-duck, controlled by the output from a

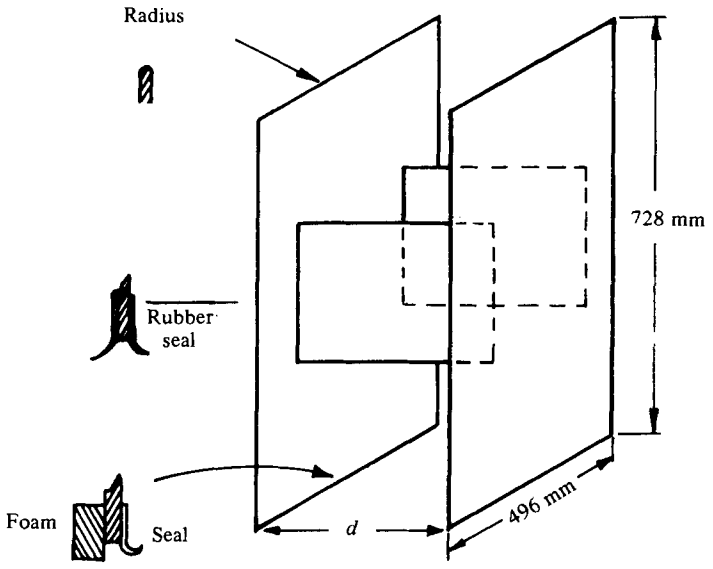

FIGURE 3. Duct fabricated from 3 mm thick mild-steel plate. d = 115, 229 and 343 mm in these experiments.

digital transfer-function analyser (Solartron 1600) which also performed the signal processing of the return signals (resolution 0·1 mV, 0·2°).

At the other end of the tank the waves were absorbed by a double-wedge absorber which reduced reflexions to less than 5 % in amplitude. The duct and the wave-measuring equipment were sited in the central area of the tank. The duct was fabricated from two 3 mm gauge steel plates bolted together by ties to produce a rigid rectangular enclosure which could be slid down into the tank and sealed to the walls and floor (figure 3).

The wave recorder was a contactless electro/mechanical device of a new design which possessed a high degree of accuracy, i.e. better than 0·3 % full scale.

One further item of equipment requires special mention, this being the pressure transducer.

3.1. *Pressure transducer*

A Gaeltec type 4T half-bridge strain transducer which had previously been adapted for underwater use was chosen for the experiment. It exhibited good sensitivity and long-term stability when operated with a.c. excitation and was found to be well suited to the application. The specifications are as follows: range, ± 200 mm water; output sensitivity, 30 mV/mm water; linearity, 0·5 %.

This differential transducer was mounted in a watertight box as illustrated schematically in figure 4. One side of the diaphragm was vented to the ambient water while the other was vented to the interior of the box, which was maintained at a virtually constant pressure. In order to eliminate adverse hydrostatic gradients across the diaphragm the internal pressure of the box was made equal to the ambient pressure in the duct via a small orifice made by the point of a pin. This ensured a slow rate of equalization such that the system acted as a high-pass filter allowing dynamic pressure measurement to be made unhindered at the frequencies of interest; the time constant was chosen to be approximately 50 s.

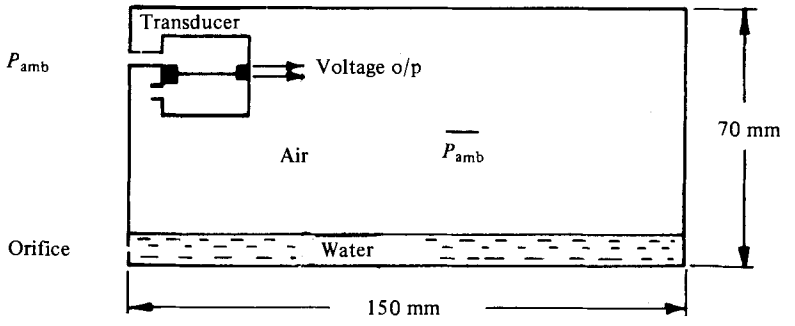

FIGURE 4. Pressure-transducer assembly (for correct operation the water level should remain above the level of the orifice).

Calibration of this instrument was effected by both static and dynamic means. The static calibration was performed by immersing the transducer to various depths with the orifice sealed and noting the change in output voltage. The accuracy of the measurements was better than 0·5 %. Dynamic calibration was effected by measuring the response of the transducer to incident long waves when it was resting on the bottom of the tank. Measurements of the incident waves and appropriate application of shallow-water theory allowed a comparison to be made between the measured and theoretical pressure fluctuations. These agreed to within 1 % in amplitude and 1·5° in phase.

4. Comments on experimental procedures

In this experiment it was essential that the pressure measured at the base of the enclosure was representative of a true 'infinite' depth pressure. This requirement was satisfied if it could be shown that the measured pressure was sensibly constant over a range of heights above the base. Two effects could introduce errors in such an arrangement. First, there was the possible influence of wave-orbital motion, and second, there was the possible influence of leakage around the walls of the enclosure, which was observed to cause attenuation of pressure fluctuations with increasing depth.

The wave-orbital activity was observed by flow-visualization techniques using fine suspended particles in the water. These motions were observed to diminish rapidly with depth within the duct and appeared to be negligible at depths below the mouth in excess of the mouth spacing itself. The influence of leakage, however, was found to be of greater importance. It was discovered that the seal between the duct and the sides and bottom of the tank had to be completely leak-tight and also hold the duct rigidly to the tank wall.

A successful seal was constructed from a combination of rubber strips and plastic foam. An indication of the importance of the leakage effect may be gauged by observing that pressure attentuation of up to 60 % was caused by occasional small gaps of about 1 mm. With the seal in its final form, a vertical traverse across the enclosure between the midpoint and the base revealed pressure variations of less than 1 %.

The second phenomenon worthy of comment concerns frictional dissipation. Measurements in an unobstructed tank indicated that freely propagating waves were attenuated by up to 2 % per metre at the wavelengths λ employed. A linear correction

Test	d_s (mm)	f (Hz)	$n = d/\lambda$	h/λ	$\lvert\zeta^+(X_A)\rvert$ (mm)
1	343	1·17	0·3	0·15	3·6
2	343	1·35	0·4	0·2	4·4
3	343	1·65	0·6	0·3	4·8
4	229	1·17	0·2	0·15	4·0
5	229	1·35	0·27	0·2	4·4
6	229	1·65	0·4	0·3	4·9
7	115	1·17	0·1	0·15	4·2
8	115	1·35	0·134	0·2	5·0
9	115	1·65	0·2	0·3	5·0
10	229	1·65	0·4	0·3	9·9

TABLE 1

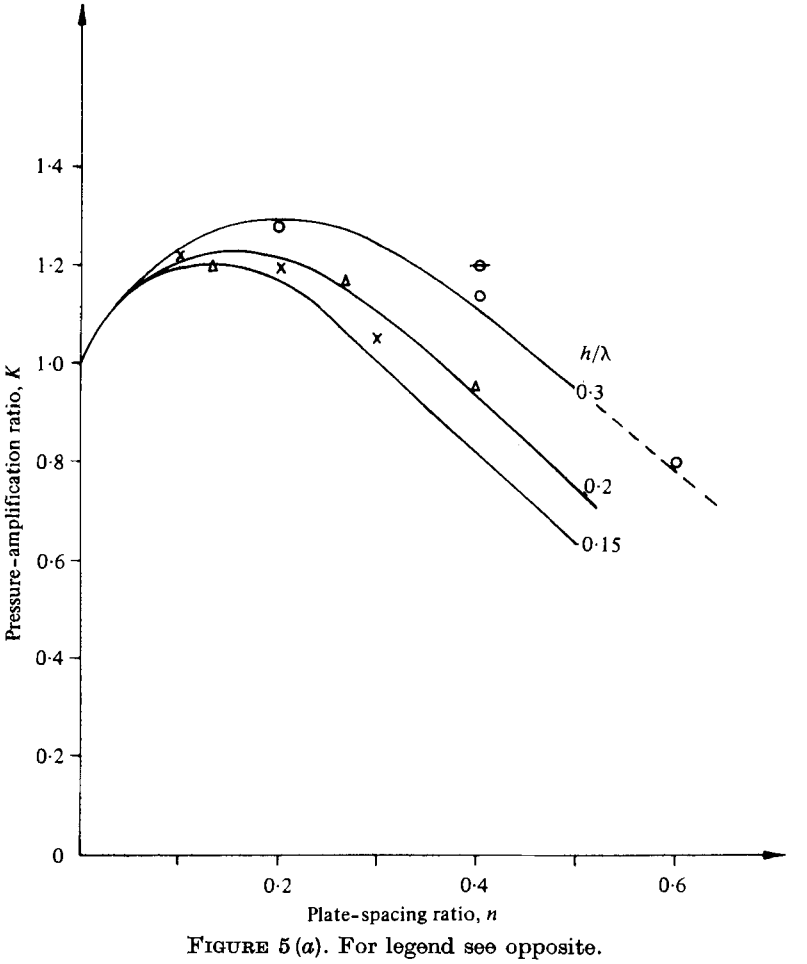

FIGURE 5 (*a*). For legend see opposite.

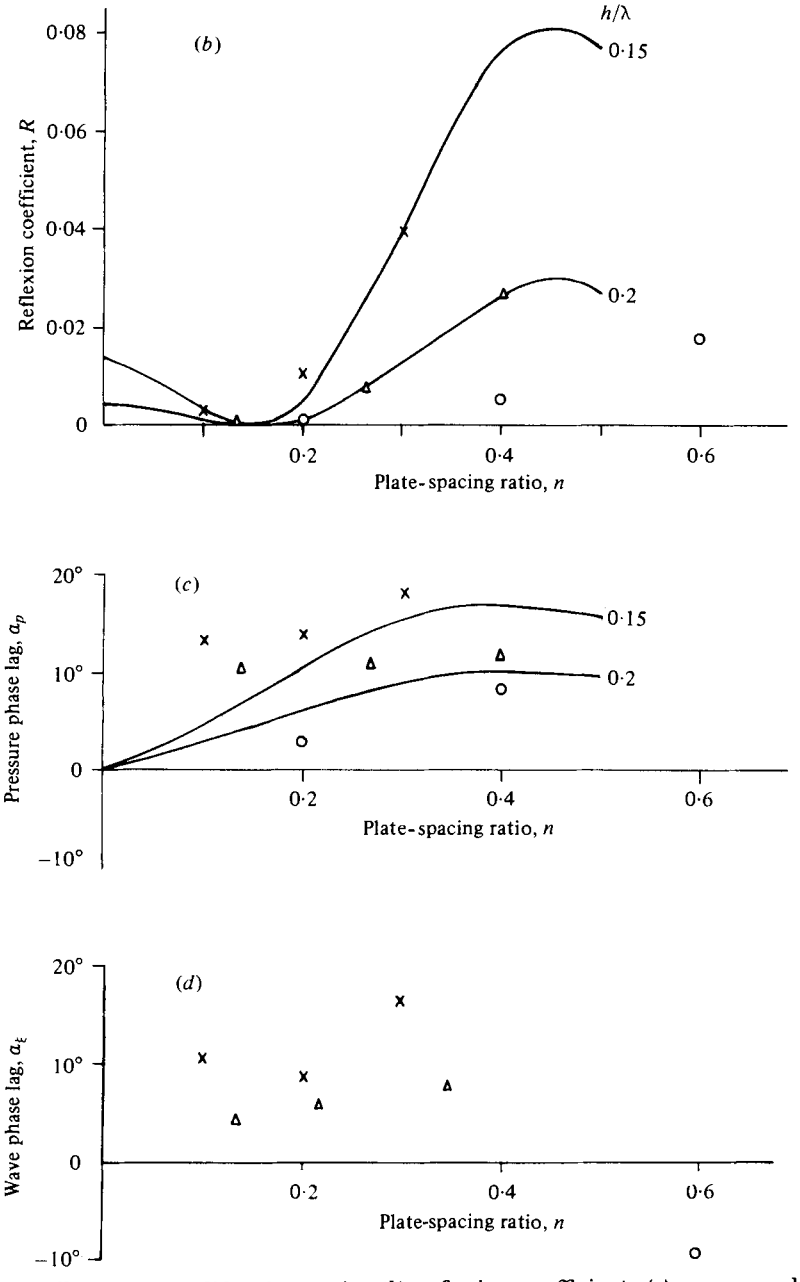

FIGURE 5. (*a*) Pressure-amplification ratio, (*b*) reflexion coefficient, (*c*) pressure phase lag and (*d*) wave phase lag. ×, $h/\lambda = 0{\cdot}15$; △, $h/\lambda = 0{\cdot}2$; ○, $h/\lambda = 0{\cdot}3$; ⊖, $h/\lambda = 0{\cdot}3$, high amplitude; ——, theory, Lighthill (1979).

for this based on wave-height measurements would have the effect of increasing the values of K and R by up to 4 %. Additional attenuation was introduced by the enclosure itself, and inspection of reflexion and transmission revealed that up to 5 % of the wave energy could be dissipated there. A linear correction for this would further increase K and R. Neither correction, however, is included in this note since their exact influence on the experiment is not known.

5. Presentation and discussion of results

Ten tests were performed, as tabulated in table 1. Nine of these were conducted with similar wave heights, and a tenth was added to observe the effect of increasing the wave height (to a steepness of $\sim \frac{1}{30}$).

The results for K, R, α_p and α_ξ are illustrated in figures 5 (*a*)–(*d*). The values of K and R deduced from the experiment are seen to compare favourably with those predicted by linear theory. The occurrence of near-zero reflexion in test 5 is of particular interest. There does appear, however, to be a consistent, if slight, trend for the pressure-amplification ratio to exceed the theoretical values, and in view of the further increase in K which occurs at the higher amplitudes it seems reasonable to associate this with nonlinear effects. These could arise either from inherent limitations in the linear theory or in the assumption of an inviscid fluid, or both.

To investigate these points, several photographs were taken of the flow about the plates, three of which are given in figure 6 (plate 1). Figure 6 (*a*) depicts the flow about the top edge of the leading plate at a wave amplitude comparable to that used in tests 1–9. Figures 6 (*b*) and (*c*) are of the same subject but at higher wave amplitudes.

Clearly, at moderate amplitudes the flow is quite well ordered, although there appears to be some separation of the flow at the top edge. At the higher amplitudes the flow is seen to separate and roll up into a strong vortex which develops somewhere behind the plate and migrates into the free stream later in the cycle. Such phenomena cannot automatically be interpreted as the cause of the observed pressure intensification but they do draw attention to the susceptibility of such experiments to boundary-layer effects and the problems which they bring to the proper scaling of results. Thus it has been considered prudent to keep perturbation amplitudes to a minimum.

6. Conclusions

This initial investigation is encouraging not only in producing values for coefficients which compare favourably with theoretical predictions, but also in confirming the existence of an appreciable amplification of duct pressures, which is of importance in the projected operation of immersed, pressure-driven, wave-energy devices. The principal query raised by this work concerns the exact behaviour of the flow in the vicinity of the plate edges and how the advent of separation limits the applicability of ideal linear theory. It seems probable that such effects will have only minor consequences unless appreciable flow in and out of the duct also occurs, in which case the creation of eddies will undoubtedly introduce further damping which could be prejudicial to efficient wave-energy conversion.

Examination of this dynamic case is thus desirable, but such a study of a fully submerged duct will involve considerable instrumentation and engineering of equipment, hence it is important to collect first the maximum information from both linear theory and 'static' flow experiments.

Complementary studies concerned with the static testing of a three-dimensional duct, together with photographic visualization of the flow at duct mouths, are currently underway, and it is to be hoped that an appropriate three-dimensional theory will be developed for these more complex situations.

The authors would like to thank their colleague Dr Malcolm Mackley for arranging the flow-visualization photography, and to acknowledge the financial assistance of the Marine Technology Directorate, S.R.C.

Appendix. Derivation of an algorithm for the directional resolution of superimposed waves

In wave-tank studies the presence of unwanted reflexions has always been a hindrance and conventionally these are accounted for by observing the standing-wave ratio and thereby deriving the amplitude of the direct and the reflected waves. In this process phase information is difficult to obtain. A mathematical algorithm is presented here for deriving the amplitudes and phases of the superimposed waves from just two, more or less arbitrarily positioned wave records. The required algebraic manipulation, although tedious to perform by hand, can easily be implemented with the aid of a programmable calculator. The results can also be used to resolve complex superimposed wave trains when Fourier analysis is employed. The latter procedure has been examined in practice and has proved to be most successful.

Formulation of the problem in two dimensions

Referring to figure 7, we have

$$\zeta^+(x) = A\sin(\omega t + kx + \phi_A), \quad \zeta^-(x) = B\sin(\omega t - kx + \phi_B), \tag{1a,b}$$

$$y(x) = \zeta^+(x) + \zeta^-(x), \tag{2}$$

where $y(x)$ is the wave record of the superimposed direct and reflected waves ζ^+ and ζ^-, whose amplitudes and phases relative to the origin and time zero are respectively A, ϕ_A, B and ϕ_B.

Two records are taken, one at $x = X_1$ and the other at $x = X_0$, which for simplicity is taken to be the origin. Translation to any other co-ordinate system can be arranged by the introduction of an appropriate phase shift. Then

$$y(X_0) = A\sin(\omega t + \phi_A) + B\sin(\omega t + \phi_B), \tag{3a}$$

$$y(X_1) = A\sin(\omega t + kX_1 + \phi_A) + B\sin(\omega t - kX_1 + \phi_B). \tag{3b}$$

These equations may be written in the form

$$y = P\cos\omega t + Q\sin\omega t, \tag{4}$$

where P and Q may be considered as the real and imaginary parts of a function varying harmonically with time. Hence the wave records may be characterized in complex notation by

$$y(X_0) = (P_0, Q_0), \quad y(X_1) = (P_1, Q_1). \tag{5a,b}$$

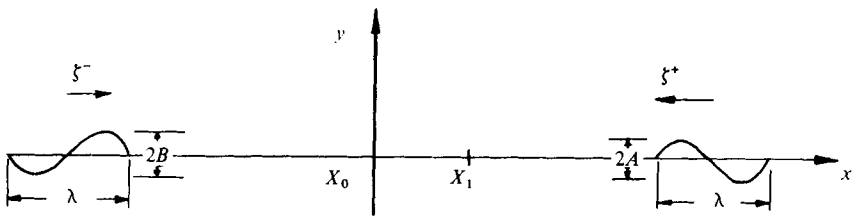

FIGURE 7. Definition of the wave system.

Expanding $(2a, b)$ and equating the real and imaginary parts to those of $(5a, b)$ gives

$$P_0 = A\sin\phi_A + B\sin\phi_B, \tag{6a}$$

$$Q_0 = A\cos\phi_A + B\cos\phi_B, \tag{6b}$$

$$P_1 = A\sin(kX_1+\phi_A) + B\sin(-kX_1+\phi_B), \tag{7a}$$

$$Q_1 = A\cos(kX_1+\phi_A) + B\cos(-kX_1+\phi_B). \tag{7b}$$

Simultaneous solution of these equations gives

$$A = \tfrac{1}{2}\{(P_0+S)^2+(Q_0+T)^2\}^{\frac{1}{2}}, \tag{8a}$$

$$B = \tfrac{1}{2}\{(P_0-S)^2+(Q_0-T)^2\}^{\frac{1}{2}}, \tag{8b}$$

$$\phi_A = \tan^{-1}\frac{P_0+S}{Q_0+T}, \quad \phi_B = \tan^{-1}\frac{P_0-S}{Q_0-T}, \tag{9a,b}$$

where

$$S = \frac{Q_0\cos kX_1 - Q_1}{\sin kX_1}, \quad T = \frac{P_1 - P_0\cos kX_1}{\sin kX_1}. \tag{10),(11}$$

Modern measurement instruments such as digital transfer function analysers often give their outputs in Cartesian as well as polar form, which conveniently allows the Cartesian coefficients P and Q to be substituted directly into the above equations. Alternatively, derivation of P and Q from amplitude and phase information is easily accomplished.

In practice, the accuracy of resolution depends on the spacing X_1. For $kX_1 = n\pi$ the solution is indeterminate, and for adjacent values it is sensitive to errors of measurement. In general, it is found to operate satisfactorily for values of kX in the interval $0{\cdot}5 < kX < 2{\cdot}5$.

REFERENCES

LIGHTHILL, M. J. 1979 Two-dimensional analyses related to wave-energy extraction by submerged resonant ducts. *J. Fluid Mech.* (to appear).

JARVIS, R. A. 1971 The scattering of surface waves by two vertical plane barriers. *J. Inst. Math. Appl.* **7**, 207–215.

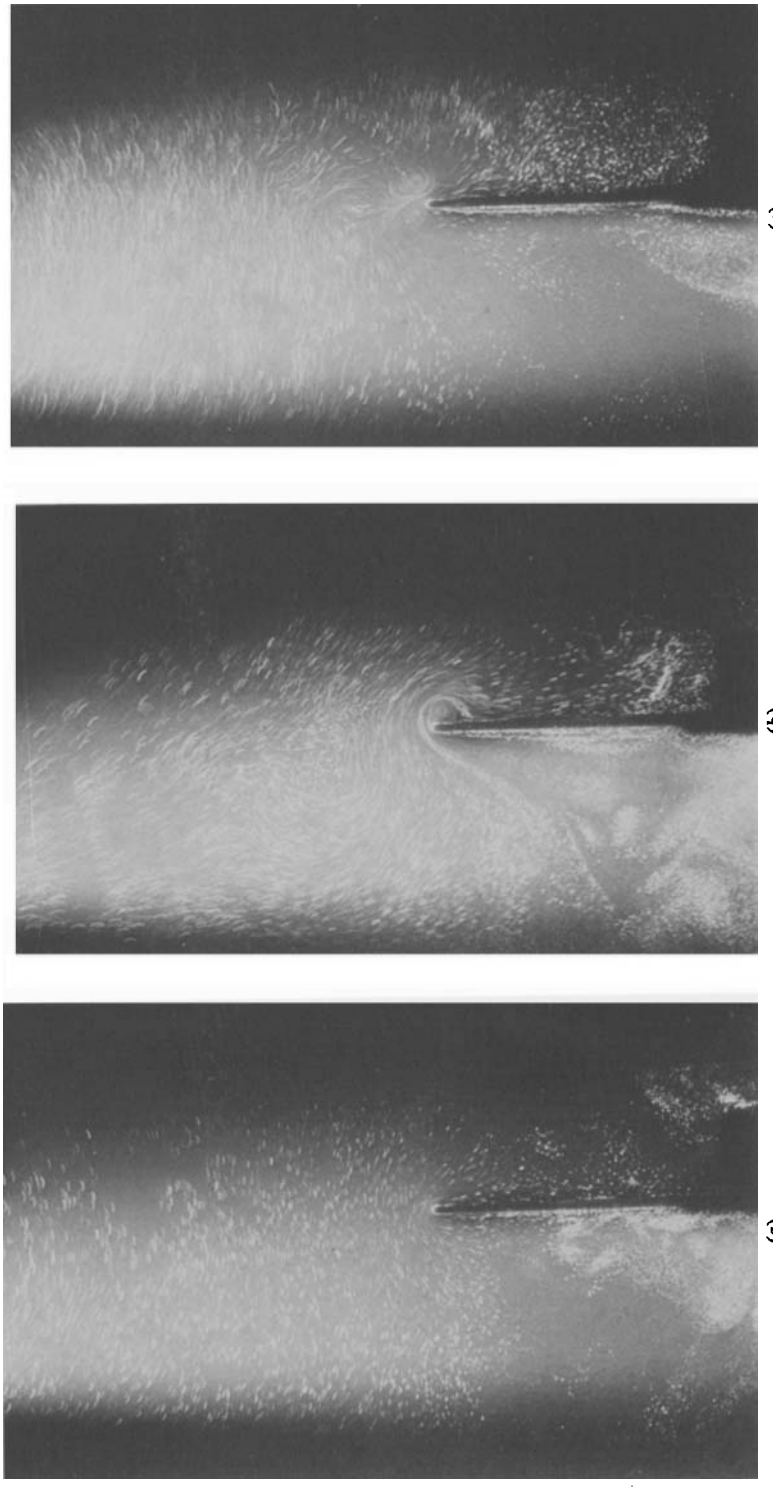

(*c*)

(*b*)

(*a*)

FIGURE 6. (*a*) Ordered flow about the leading plate at low wave amplitude, $f = 1{\cdot}35$ Hz, $|\zeta^+| = 4$ mm. (*b*) Vortex formation behind leading plate at increased amplitude, $f = 1{\cdot}35$ Hz, $|\zeta^+| = 8$ mm. (*c*) Separation of the vortex from the edge of the plate, $f = 1{\cdot}35$ Hz, $|\zeta^+| = 12$ mm.